International Journal of the Physical Sciences Vol. 6(26), pp. 6166-6170, 30 October, 2011
Available online at http://www.academicjournals.org/IJPS
DOI: 10.5897/IJPS11.500
ISSN 1992-1950 ©2011 Academic Journals

Full Length Research Paper

The period effects of intraperitoneal administration of different gold nanoparticle sizes on heart tissue of rats using fluorescence measurements: *In vivo*

Mohamed Anwar K. Abdelhalim

Department of Physics and Astronomy, College of Science, King Saud University, P. O. 2455, Riyadh 11451, Kingdom of Saudi Arabia. E-mail: abdelhalimmak@yahoo.com, mabdulhleem@ksu.edu.sa.

Accepted 14 July, 2011

Despite many benefits of nanotechnology, some studies indicate that certain nanoparticle (NPs) may cause adverse effects because of their small size and unique properties. The aim of the present study was to elucidate the period effects of intraperitonealy administration of different gold nanoparticle sizes on rat heart tissue *in vivo* using fluorescence spectroscopy. The experimental rats were divided into control and six groups (G1A, G1B, G2A, G2B, G3A and G3B; G1: 20 nm; G2: 10 nm; G3: 50 nm; A: infusion of GNPs for 3 days; B: infusion of GNPs for 7 days). To investigate the period effects of gold nanoparticles (GNPs) 10, 20 and 50 nm on the heart tissue of rats, 50 µl dose of GNPs (of concentration 0.1% Au) were intraperitonealy injected into rats for periods of 3 and 7 days to identify the toxicity and tissue distribution of GNPs *in vivo* using fluorescence measurements. The high electron densities of GNPs as well as the homogeneity of the particles shape and size make them highly conspicuous under the transmission electron microscope (TEM). The peak fluorescence intensity increased for G1B compared with G1A, increased for G2B compared with G2A and sharply decreased for G3A and G3B compared with the control. The peaks of G1A, G1B, G2A, G2B, G3A and G3B shifted towards the UV-Visible wavelength compared with the control. The peak fluorescence intensity for G1A was higher than G2A, G3A and G3B while G2A was higher than G3A. The peak fluorescence intensity for G2B was higher than G1B and G3B while G1B was higher than G3B. GNPs of sizes 10 and 20 nm have spherical shape while GNPs of size 50 nm have hexagonal shape. Fluorescence intensity of GNPs was size, shape and infusion period dependent. The decrease in peak fluorescence intensity induced in large 50 nm GNPs may be attributed to occurrence of quenching, decrease number and surface area of GNPs in addition to high clearance of GNPs via urine and bile. Moreover, decreasing size may lead to an exponential increase in surface area relative to volume, thus making the GNPs surface more reactive on itself (aggregation) and to its surrounding environment (biological components). Size, shape, surface area, number and clearance of GNPs play a key role in toxicity, and alterations of accumulation of GNPs in the heart tissue which may be mediated by dynamic protein binding and exchange. A better understanding of these mechanisms will improve drug delivery.

Key words: Gold nanoparticles, sizes, administration period, heart tissue, fluorescence spectroscopy.

INTRODUCTION

Fluorescence has many practical applications, including mineralogy, gemology, chemical sensors, fluorescent labelling, dyes and biological detectors. Fluorescence is the emission of light by a substance that has absorbed light or other electromagnetic radiation of a different wavelength. In most cases, emitted light has a longer wavelength, and therefore lower energy, than the absorbed radiation. However, when the absorbed electromagnetic radiation is intense, it is possible for one electron to absorb two photons; this two-photon absorption can lead to emission of radiation having a shorter wavelength than the absorbed radiation. Size, surface area and number of NPs appear to play important roles in facilitating nano-sized particle-related toxicity. It

had been proposed that the size of the particles plays a key role in their adhesion to and interaction with biological cells (Foster et al., 1997).

The origin of the unique optical properties of (GNPs) is a phenomenon known as surface plasmon resonance (SPR). When an electromagnetic radiation, of a wavelength much smaller than the diameter of the GNPs, hits the particles, it induces coherent, resonant oscillations of the metal electrons across the nanoparticles. These oscillations are known as the SPR, which lie within visible frequencies and result in strong optical absorbance and scattering properties of the GNPs (Schmid, 1992; Jain et al., 2007). This property allows the use of GNPs for many applications, e.g., they can be used as Raman sensors (Tian et al., 2002), photocatalysts (Kamat, 2002), and photoelectrochemical materials (Shipway et al., 2000). In the bioscience and medical fields, GNPs are used as immunostaining marker particles for electron microscopy, and as chromophores for immunoreactions and nucleic acid hybridization (Mirkin et al., 1996; Huber et al., 2004).

Numerous studies have showed that exposures to nanoscale particles produce greater inflammatory and cytotoxic effects when compared to exposures to larger sized particles at equivalent mass concentration (Schmid, 1992; Wang et al., 2007). It is considered that nanoparticles can be more reactive with biological components and have adverse effects due to large surface area and much particle number (Nel et al., 2006). Toxicity has been thought to originate from nanomaterial size and surface area, composition, and shape. Size plays a role in how the body responds to, distributes, and eliminates materials (Kamat, 2002; Huber et al., 2004). Particle size can also affect the mode of endocytosis, cellular uptake, and the efficiency of particle processing in the endocytic pathway (Liu, 2006; Baptista et al., 2008).

GNPs can be used in various biomedical applications, however, very little is known about their size-dependent *in vivo* kinetics. Here we focus our attention on aspects related to fluorescence spectroscopy for different GNP sizes dissolved in aqueous solution. Moreover, the particles size and shape were monitored by the transmission electron microscopy. Thus, the aim of the present study was to elucidate the period effects of intraperitonealy administration of different GNP sizes on the rat heart tissue *in vivo* using fluorescence spectroscopy.

MATERIALS AND METHODS

Gold nanoparticles (GNPs)

Different GNP sizes of 10, 20 and 50 nm were purchased (Product MKN-Au-010, MKN-Au-020 and MKN-Au-050 in aqueous solution of concentration 0.01% of gold, Canada) and used in this study.

The mean size and morphology with good particle size distribution for these GNPs were calculated from the images taken by the transmission electron microscope (TEM). In addition to the assessment are the high electron densities of GNPs as well as the homogeneity of the particles shape and size.

Animals

Healthy, male Wistar-Kyoto rats were obtained from the Laboratory Animal Center (College of Pharmacy, King Saud University). 8 to10 weeks old (approximately 250 g body weight) were housed in pairs in humidity and temperature-controlled ventilated cages on a 12 h day/night cycle. A rodent diet and water were provided. To study the infusion period effects of GNP size, forty four rats were individually caged, and divided into control group (NG: n = 8), Group 1 (G1A: Infusion of GNPs of size 20 nm for 3 days; n = 6 and G1B: Infusion of GNPs of size 20 nm for 7 days; n = 6), Group 2 (G2A: Infusion of GNPs of size 10 nm for 3 days; n = 6 and G2B: infusion of GNPs of size 10 nm for 7 days; n = 6) and group 3 (G3A: Infusion of GNPs of size 50 nm for 3 days; n = 6 and G3B: Infusion of GNPs of size 50 nm for 3 days; n = 6). All experiments were conducted in accordance with the guidelines approved by King Saud University Local Animal Care and Use Committee. 10, 20 and 50 nm GNPs in aqueous solutions was intraperitonealy administered to the animals. The rats were anesthetized by inhalation of 5% isoflurane until muscular tonus relaxed.

Digestion of heart rat tissue samples

Heart rat tissue samples were wet digested with nitric acid and converted into acidic digest solutions for analysis by fluorescence spectroscopy. The tissue was freeze dried in order to minimize loss of analytes and to facilitate subsequent sample preparation steps, and then homogenized to a fine powder by ball-milling in plastic containers. Approximately 0.20 to 0.25 g of powdered tissue was weighed into a Teflon reaction vessel and 3 ml of HNO_3 were added. The closed reaction vessel was heated in a 130°C oven until digestion was completed. Samples were then diluted to a final volume of 20 ml with quartz distilled water and stored in 1 oz. polyethylene bottles for later fluorescence spectroscopy analysis.

Fluorescence spectroscopy

Fluorescence characterization of different GNP sizes (10, 20 and 50 nm) was performed using FluoroMax-2 (JOBIAN YVON-SPEX, Instruments S.A., Inc., France). Fluorescence measurements were made over the wavelength range of 250 to 700 nm. The fluorescence measurements were made using 1 cm path length quartz cuvettes which were cleaned before each use by sonicating them for 5 min in deionized water and then rinsing with deionized water.

RESULTS AND DISCUSSION

Size and morphology of different GNPs size

The GNPs sizes 10 and 20 nm show spherical morphology with good particle size distribution dispersed in the solution. The mean sizes for these GNPs were calculated from the images taken by the TEM. Mean size was 9.45 ± 1.33 nm for GNPs of size 10 nm and 20.18 ± 1.80 nm for GNPs of size 20 nm while GNPs of 50 nm have hexagonal shape. The high electron densities of

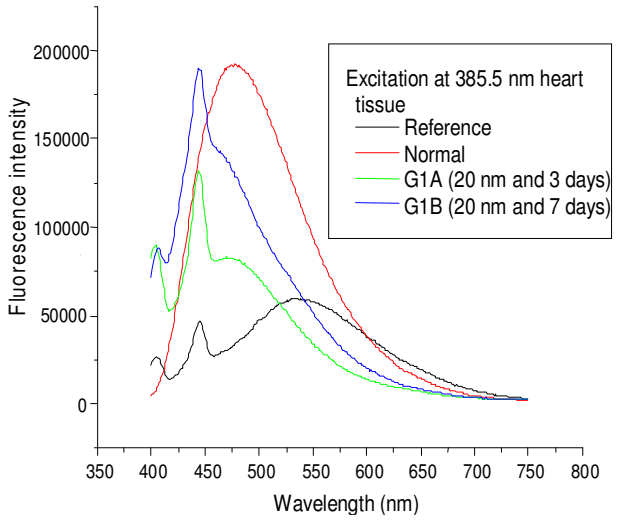

Figure 1. The emission fluorescence peak intensity for GNP of size 20 nm at infusion periods of 3 and 7 days.

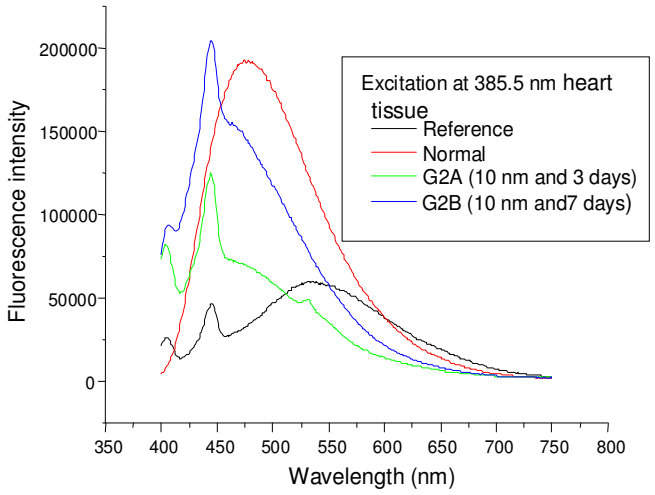

Figure 2. The emission fluorescence peak intensity for GNPs of size 20 nm at infusion periods of 3 and 7 days.

GNPs as well as the homogeneity of the particles shape and size make them highly conspicuous under the TEM. The results of Figures 1 and 2 show that the peaks fluorescence intensity increased for G1B compared with G1A and for G2B compared with G2A, and peaks of G1A, G1B, G2A and G2B shifted towards the UV-Visible wavelength compared with the control. This demonstrates that the increase in fluorescence intensity is GNPs administration period dependent.

Figure 3 shows that the peaks fluorescence intensity sharply decreased for G3A and G3B compared with the control, and the peaks shifted towards the UV-Visible wavelength compared with the control. The peak fluorescence intensity for G3A was higher than G3B.

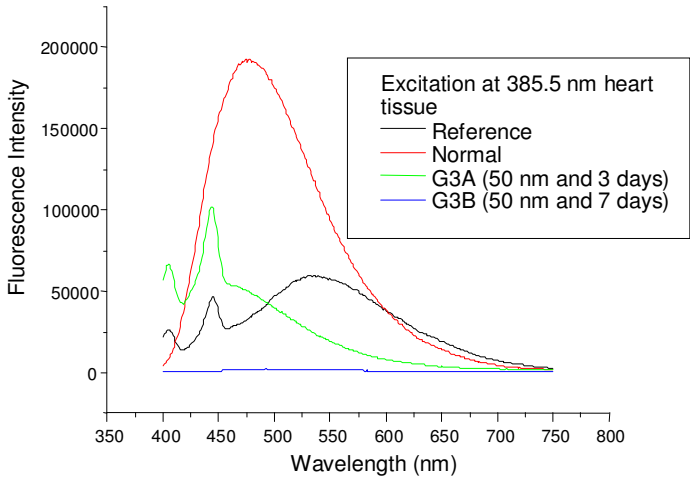

Figure 3. The emission fluorescence peak intensity for GNPs of size 50 nm at infusion periods of 3 and 7 days.

Figure 4 shows that the peak fluorescence intensity sharply decreased for G1A, G2A and G3A compared with the control, and these peaks shifted towards the UV-Visible wavelength compared with the control. The peak fluorescence intensity for G1A was higher than G2A and G3A, and G2A was higher than G3A.

This sharp decrease in the peak fluorescence intensity compared with the control may be attributed to the following: (1) The occurrence of a strong quenching of the fluorescence from serum albumins due to the formation of a ground state complex with GNPs (static quenching); (2) Electron microscopy revealed that most GNPs of size 50 nm were of hexagonal morphology than spherical morphology (GNPs of sizes 10 and 20 nm); (3) The physical and chemical properties as well as the applications of NPs are controlled and limited by their dimensions and shape; (4) The 50 nm GNPs may be taken up faster and more intensively than the other sizes by macrophages of the heart and disappeared thereafter. The emission fluorescence peak intensity for 10, 20 and 50 nm GNPs at infusion period of 3 days.

Figure 5 shows that the peak fluorescence intensity increased for G2B, nearly the same for G1B and sharply decreased for G3B compared with the control, and these peaks shifted towards the UV-visible wavelength compared with the control. The peak fluorescence intensity for G2B was higher than G1B and G3B, and G1B was higher than G3B.

Figure 6 shows that the peak fluorescence intensity increased for G2B, nearly the same for G1B and sharply decreased for G1A, G2A, G3A and G3B compared with the control, and these peaks shifted towards the UV-visible wavelength compared with the control. The peak fluorescence intensity for G1A was higher than G2A, G3A and G3B, and G2A was higher than G3A. The peak fluorescence intensity for G2B was higher than G1B and G3B, and G1B was higher than G3B.

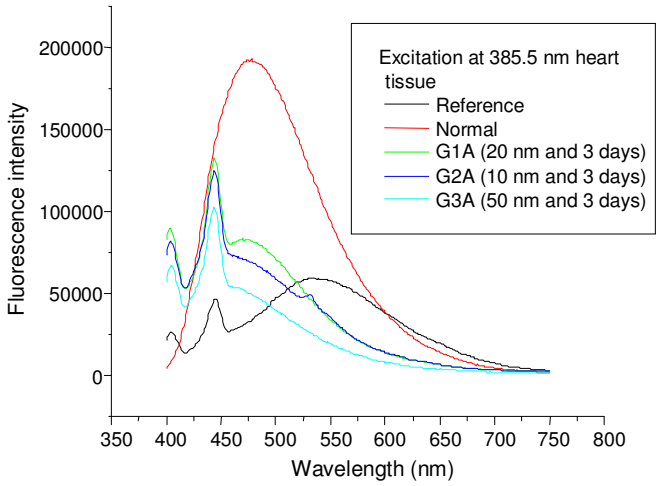

Figure 4. The emission fluorescence peak intensity for GNP of sizes 10, 20 and 50 nm at infusion period of 3 days.

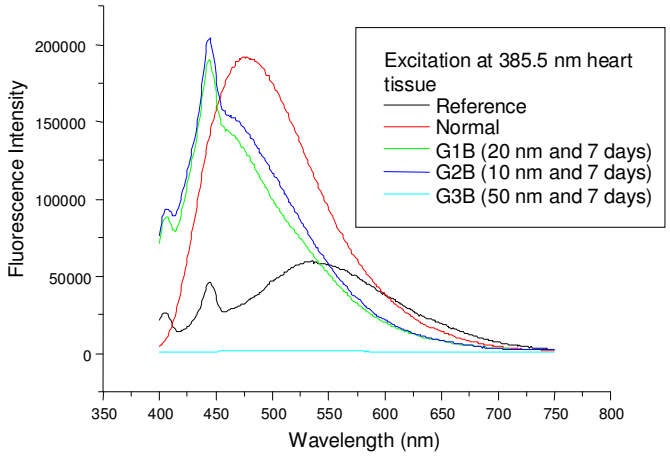

Figure 5. The emission fluorescence peak intensity for GNP of sizes 10, 20 and 50 nm at infusion period of 7 days.

This result indicates that decreasing GNP size may lead to an exponential increase in surface area relative to volume, thus making the GNPs surface more reactive on itself (aggregation) and to its surrounding environment (biological components). This study suggests that the increase in fluorescence intensity may be attributed to increased accumulation of GNPs in the tissues in addition to slow clearance via urine and bile. Increased uptake into certain tissues may lead to accumulation, where they may interfere with critical biological functions (Liu, 2006; Shrestha et al., 2006). The rate of exocytosis of GNPs was size dependent with more accumulation of larger GNPs in the cell (Shrestha et al., 2006).

It had been published that GNPs of very small sizes impart physical and chemical properties that are very different from those of the same material in the bulk form. These properties include a large surface to volume ratio,

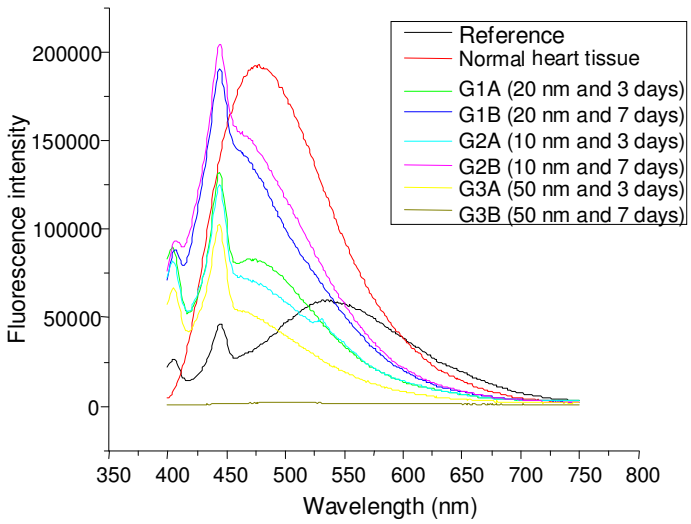

Figure 6. The emission fluorescence peak intensity for GNP of sizes 10, 20 and 50 nm at infusion periods of 3 and 7 days.

enhanced or hindered particle aggregation depending on the type of surface modification, enhanced photo-emission, high electrical and heat conductivity, and improved surface catalytic activity (Liu, 2006; Shrestha et al., 2006).

Since this surface area can interact with biological components of cells, small NPs can be more reactive *in vivo* than larger particles. Incidence and severity of inflammatory response was transiently increased with injection of 200 and 100 nm GNPs within 12 h. GNPs were trapped by macrophages in the spleen and heart and remained there until 4 weeks after the single injection (Cho et al., 2010).

To evaluate the impact of a particle size on tissue distribution, we injected 50 µl of 10, 20 and 50 nm GNPs daily for periods of 3 and 7 days. The 50 nm GNPs were taken up faster and more intensively than the other sizes by macrophages of the heart and disappeared thereafter. This result is related with the inflammatory response of the heart.

NPs for therapy need to have a long retention time for targeting and therapy. However, a long retention time can evoke the toxic effects *in vivo.* Thus, the clearance rate and route of nanomaterials is an important issue (Cho et al., 2010; Choi et al., 2007).

Absorbed NPs within the systemic circulation can be excreted through various routes. A possible elimination route for NPs could be renal and biliary clearance. Renal clearance of solid nano-sized materials was affected by particle size and surface charge (Choi et al., 2007; Gupta, 2005).

In our study, we compared peak fluorescence intensity for GNPs of varying particle size after intraperitonealy injection into rats for periods of 3 and 7 days. It has been demonstrated that fluorescence intensity and heart tissue distribution was different depending on particle size. The

fluorescence intensity for 10 and 20 nm GNPs increased with the increase of the infusion period of GNPs from 3 to 7 days while it decreased for 50 nm GNPs. As particle sizes increased, fluorescence intensity decreased because more particles were trapped by macrophages. These results could serve as a guideline in the rational design of drug nanocarriers with maximized therapeutic efficacy and predictable *in vivo* properties, in which the control of particle size and shape was of significance.

All injected GNPs showed a propensity to accumulate in the rat heart tissue. The heart tissue distribution of GNPs is size-dependent, with the smallest particles showing the most widespread organ distribution. Smaller GNPs showed greater cellular accumulation due to the dose-metric treatment. Therefore, GNPs target organs with many phagocytic cells such as liver, spleen, lung, kidney and mesenteric lymph node should be taken into consideration.

Conclusions

The aim of the present study was to elucidate the period effects of intraperitonealy administration of different gold nanoparticle sizes (10, 20 and 50 nm) on the heart tissue of rats using fluorescence measurements in *vivo*.

The high electron densities of GNPs as well as the homogeneity of the particles shape and size make them highly conspicuous under the TEM. GNPs of sizes 10 and 20 nm have spherical shape while GNPs of size 50 have hexagonal shape.

After intraperitonealy injection of 10, 20 and 50 nm GNPs into the experimental rats, peak fluorescence intensity increased for G1B compared with G1A, increased for G2B compared with G2A and sharply decreased for G3A and G3B compared with the control. The peaks of G1A, G1B, G2A, G2B, G3A and G3B shifted towards the UV-visible wavelength compared with the control. This study demonstrates that peak fluorescence intensity of GNPs was size, shape, number, surface area and infusion period dependent of GNPs.

The decrease in fluorescence intensity induced in large 50 nm GNPs may be attributed to occurrence of quenching, decrease number and surface area of GNPs in addition to highly clearance of GNPs via urine and bile. Moreover, decreasing size may lead to an exponential increase in surface area relative to volume, thus making GNPs surface more reactive on itself (aggregation) and to its surrounding environment (biological components). Size, shape, surface area, number and clearance of GNPs play a key role in toxicity, and alterations of accumulation of GNPs in the heart tissue which may be mediated by dynamic protein binding and exchange. A better understanding of these mechanisms will improve drug delivery.

This study suggests that additional further experiments in several organs of rats are needed to support the application of GNPs as a therapeutic and diagnostic tool.

ACKNOWLEDGEMENTS

The author is very grateful to NPST. This research was financially supported by the National Science and Technology Innovation Plan (NSTIP), Research No. 08-ADV206-02 and Research No. 09-NAN670-02, College of Science, King Saud University, Saudi Arabia.

REFERENCES

Baptista P, Pereira E, Eaton P, Doria G, Miranda A, Gomes I, Quaresma P, Franco R (2008). Gold nanoparticles for the development of clinical diagnosis methods. Anal. Bioanal. Chem., 391: 943-50.

Cho WS, Cho M, Jeong j, Choi M, Han BS, Shin HS, Hong J, Chung BH, Jeong J, Cho MH (2010). Size-dependent tissue kinetics of PEG-coated gold nanoparticles. Toxicol. Appli. Pharmacol., 245: 116–123.

Choi CJ, Anantharam V, Saetveit NJ, Houk RS, Kanthasamy A, Kanthasamy AG (2007). Control Cellular Prion Protein Protects against Manganese-induced Oxidative Stress and Apoptotic Cell Death. Section: Neurotoxicology, 52(3): 3-280.

Foster W, Ruka M, Gareau P, Foster RA, Janzen EG, Yang JZ (1997). Morphologic characteristics of endometriosis in the mouse model: application to toxicology. Can. J. Phsiol. Pharmacol., 75(10-11): 1188-1196.

Gupta R (2005). System behaviour of wood truss assemblies. Progress Struct. Eng. Mate., 7(4): 183-193.

Huber M, Wei TF, Muller UR, Lefebvre PA, Marla SS, Bao YP (2004). PEG-modified gold nanorods with a stealth character for in vivo applications. Nucleic Acids Res., 32: e137–e145.

Jain P, El-Sayed I, El-Sayed M (2007). Au nanoparticles target cancer. Nano Today 2: 18-29.

Kamat PV (2002). Photophysical, Photochemical and Photocatalytic Aspects of Metal Nanoparticles. J. Phys. Chem. B., 106: 7729–7744.

Liu WT (2006). Nanoparticles and their biological and environmental applications. J. Biosci. Bioeng., 102: 1–7.

Mirkin CA, Letsinger RL, Mucic RC, Storhoff JJ (1996). A DNA-based assembling nanoparticles into macroscopic materials. Nature 382: 607–609.

Nel A, Xia T, Mädler L, Li N (2006). Toxic Potential of Materials at the Nanolevel. Science. 311: 622-627.

Schmid G (1992). Large clusters and colloids. Metals in the embryonic state, Chem. Rev., 92: 1709.

Shipway AN, Eugenii K, Itamar W (2000). Nanoparticle arrays on surfaces for optical, and sensor applications. Chem. Phys. Chem., 1: 18–52.

Shrestha S, Yeung C, Nunnerley C, Tsang S (2006). Comparison of morphology and electrical conductivity of various thin films containing nano-crystalline praseodymium oxide particles. Sens. Actuators A. Phys., 136: 8-191.

Tian ZQ, Bin R, Wu DY (2002). Surface-enhanced Raman scattering: From noble to surfaces to ordered nanostructures. J. Phys. Chem. B., 106: 9463–9483.

Wang X, Duan S, Geng B, Cui J, Yang Y (2007). A missing link to angiosperms? BMC Evolutionary Biol., 7: 1-13.